

1-1-2002

Identification of Omi/HtrA-2 as a mitochondrial apoptotic serine protease that disrupts inhibitor of apoptosis protein-caspase interaction

Ramesh Hegde

Srinivasa M. Srinivasula

Zhi-Jia Zhang

Richard Wassell

Rula Mukattash

For similar works, visit stars.library.ucf.edu/facultybib2000

University of Central Florida Libraries <http://library.ucf.edu>

This Article is brought to you for free and open access by the Faculty Bibliography at STARS. It has been accepted for inclusion in Faculty Bibliography 2000s by an authorized administrator of STARS. For more information, please contact STARS@ucf.edu.

Recommended Citation

Hegde, Ramesh; Srinivasula, Srinivasa M.; Zhang, Zhi-Jia; Wassell, Richard; Mukattash, Rula; Cilenti, Lucia; DuBois, Garrett; Lazebnik, Yuri; Zervos, Anthonis S.; Fernandes-Alnemri, Teresa; and Alnemri, Emad S., "Identification of Omi/HtrA-2 as a mitochondrial apoptotic serine protease that disrupts inhibitor of apoptosis protein-caspase interaction" (2002). *Faculty Bibliography 2000s*. 3251.
<https://stars.library.ucf.edu/facultybib2000/3251>

Authors

Ramesh Hegde, Srinivasa M. Srinivasula, Zhi-Jia Zhang, Richard Wassell, Rula Mukattash, Lucia Cilenti, Garrett DuBois, Yuri Lazebnik, Anthonis S. Zervos, Teresa Fernandes-Alnemri, and Emad S. Alnemri

Identification of Omi/HtrA2 as a Mitochondrial Apoptotic Serine Protease That Disrupts Inhibitor of Apoptosis Protein-Caspase Interaction*

Received for publication, October 9, 2001, and in revised form, October 17, 2001
Published, JBC Papers in Press, October 17, 2001, DOI 10.1074/jbc.M109721200

Ramesh Hegde^{‡§}, Srinivasa M. Srinivasula^{‡§¶}, ZhiJia Zhang[‡], Richard Wassell[‡],
Rula Mukattash[‡], Lucia Cilenti^{||}, Garrett DuBois[‡], Yuri Lazebnik^{**}, Antonis S. Zervos^{||},
Teresa Fernandes-Alnemri[‡], and Emad S. Alnemri^{‡‡}

From the [‡]Center for Apoptosis Research and the Department of Microbiology and Immunology, Kimmel Cancer Institute, Thomas Jefferson University, Philadelphia, Pennsylvania 19107, ^{**}Cold Spring Harbor Laboratory, Cold Spring Harbor, New York 11724, and the ^{||}Biomolecular Research Center and Department of Molecular Biology and Microbiology, University of Central Florida, Orlando, Florida 32826

To identify human proteins that bind to the Smac and caspase-9 binding pocket on the baculoviral inhibitor of apoptosis protein (IAP) repeat 3 (BIR3) domain of human XIAP, we used BIR3 as an affinity reagent, followed by elution with the BIR3 binding peptide AVPIA, microsequencing, and mass spectrometry. The mature serine protease Omi (also known as HtrA2) was identified as a mitochondrial direct BIR3-binding protein and a caspase activator. Like mature Smac (also known as Diablo), mature Omi contains a conserved IAP-binding motif (AVPS) at its N terminus, which is exposed after processing of its N-terminal mitochondrial targeting sequence upon import into the mitochondria. Mature Omi is released together with mature Smac from the mitochondria into the cytosol upon disruption of the outer mitochondrial membrane during apoptosis. Finally, mature Omi can induce apoptosis in human cells in a caspase-independent manner through its protease activity and in a caspase-dependent manner via its ability to disrupt caspase-IAP interaction. Our results provide clear evidence for the involvement of a mitochondrial serine protease in the apoptotic pathway, emphasizing the critical role of the mitochondria in cell death.

caspase activation by binding to the BIR domain of IAPs and disrupting IAP-caspase interaction (5–7). Although Smac/Diablo does not share sequence homology with these proteins except for the first four N-terminal residues, which constitute its IAP-binding motif (8, 9), it is the only known mammalian functional homolog of these proteins with a similar mode of action. Smac promotes caspase activation and apoptosis by binding to the BIR3 and BIR2 domains of XIAP and disrupting its interaction with caspase-9 and the effector caspases (caspase-3 and -7) (8–10). Since the mechanism of IAP inhibition of caspases is conserved in mammals and insects, it is expected that other mammalian IAP-binding proteins are still undiscovered. In this report, we identified the serine protease Omi/HtrA2 as a mitochondrial direct IAP-binding protein, which is released from the mitochondria upon induction of apoptosis by apoptotic stimuli. Like Smac, the mature Omi protein contains a conserved IAP-binding motif (AVPS) at its N terminus. We demonstrate that deregulated expression of Omi in the cytoplasm of mammalian cells induces apoptosis in these cells, indicating that Omi could participate in the mitochondrial apoptotic pathway.

EXPERIMENTAL PROCEDURES

Affinity Purification of Omi from Human 293 Cells—5 ml of 293 cell pellet was washed once in phosphate-buffered saline (10 mM phosphate, pH 7.4, containing 150 mM NaCl) and centrifuged, and the pellet was resuspended in 10 ml of cell lysis buffer (20 mM Tris-HCl, pH 7.4, 150 mM NaCl, 1 mM dithiothreitol, 1 mM EDTA, 1 mM EGTA supplemented with protease inhibitor mix (Sigma P-8340) containing 4-(2-aminoethyl)-benzenesulfonyl fluoride, pepstatin A, E-64, bestatin, leupeptin, and aprotinin). Cells were homogenized and centrifuged once at 20,000 × g, and the supernatant was then subjected to centrifugation at 100,000 × g. The resultant supernatant was precleared with glutathione-Sepharose beads and then incubated with GST-BIR3 bound to glutathione-Sepharose beads for 12 h at 4 °C. The mixture was centrifuged at 500 rpm for 3 min, and the GST-BIR3 bead pellet was washed three times in the lysis buffer. The GST-BIR3-bound proteins were eluted with 200 μM AVPIA-Smac peptide at 37 °C for 1 h and then analyzed by Far Western blotting with ³⁵S-labeled *in vitro* translated XIAP as described below.

cDNA Cloning and Expression of Recombinant Proteins—The full-length human Omi cDNA clone was obtained from the IMAGE consortium (GenBank™ accession number AI979237). Constructs encoding full-length Omi or truncated mutants were generated by PCR using modified complementary PCR adapter primers. C-terminal FLAG epitope tagging was done by cloning the PCR-generated Omi cDNAs in frame into FLAG-C-pCDNA3. Plasmids encoding GFP fusion proteins were constructed using pEGFP-N1 (CLONTECH). Full-length XIAP and its BIR3-RING (residues 243–497) domain were overexpressed in *E. coli* strain DH5α as N-terminally GST-tagged proteins using a pGEX 4T vector (Amersham Biosciences, Inc.). Full-length XIAP, cIAP1, and

The IAP¹ proteins were first identified from baculoviruses as proteins that function to suppress host cell death upon viral infection (1). More recently, IAPs were found in mammals, insects, nematodes, and yeast (1–3). All IAPs share one or more signature motifs, referred to as BIRs, that are essential for the antiapoptotic activity associated with these proteins. The BIR motifs have been shown to bind directly to caspases and to inhibit their activity (2, 4). In the insect *Drosophila melanogaster*, three proteins known as Reaper, Hid, and Grim have been identified as direct IAP-binding proteins that promote

* This work was supported by National Institutes of Health Grants AG13487 and CA78890 (to E. S. A.). The costs of publication of this article were defrayed in part by the payment of page charges. This article must therefore be hereby marked “advertisement” in accordance with 18 U.S.C. Section 1734 solely to indicate this fact.

§ These two authors contributed equally to this work.

¶ Special Fellow of the Leukemia and Lymphoma Society.

‡‡ To whom correspondence should be addressed: Thomas Jefferson University, Kimmel Cancer Institute, Bluemle Life Sciences Building, Rm. 904, 233 S. 10th St., Philadelphia, PA 19107. Tel.: 215-503-4632; Fax: 215-923-1098; E-mail: E_Alnemri@lac.jci.tju.edu.

¹ The abbreviations used are: IAP, inhibitor of apoptosis protein; BIR, baculoviral IAP repeat; GST, glutathione S-transferase; GFP, green fluorescent protein; RFP, red fluorescent protein.

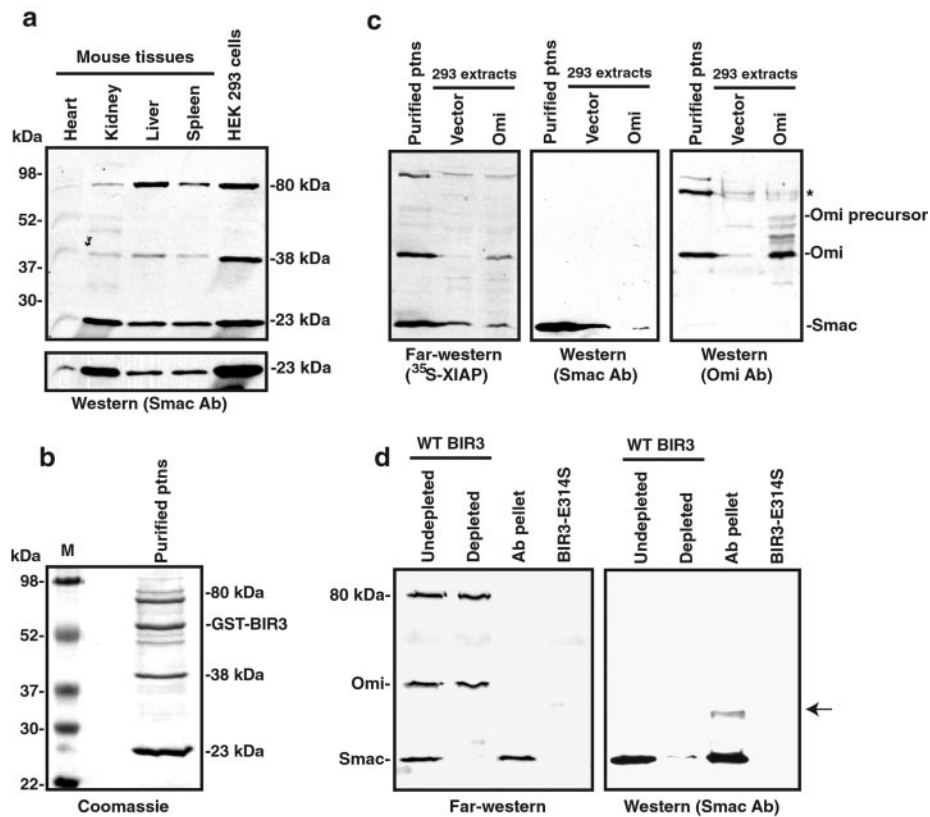


FIG. 1. Identification of Omi as a BIR3-binding protein. *a*, extracts from HEK293 cells or mouse heart, kidney, liver, or spleen tissues were bound to GST-BIR3 fusion protein, and the bound proteins were eluted with the Smac AVPIA peptide. The AVPIA peptide eluates were fractionated by SDS-PAGE and then Far Western blotted with ³⁵S-labeled XIAP (upper panel) or immunoblotted with a Smac monoclonal antibody (lower panel). *b*, Coomassie-stained gel of the GST-BIR3 affinity-purified proteins. The 23-, 38-, and 80-kDa bands were excised from the gel and subjected to automated microsequencing followed by mass spectrometry. The band immediately below the 80-kDa band was identified as Hsp70. *c*, 293-T cells were transfected with an Omi precursor expression construct (*Omi* lane) or empty vector (*vector* lane), and their extracts were fractionated by SDS-PAGE and then Far Western blotted with ³⁵S-labeled XIAP (*left* panel) or immunoblotted with Smac antibody (*middle* panel) or an Omi polyclonal antibody (*right* panel). *First* lane, GST-BIR3 affinity-purified proteins from 293 cells. A small amount of the unprocessed Omi precursor protein can be seen in the *Omi* lane. *d*, 293 cellular extracts were either left untreated (*Undepleted* lane) or depleted with Smac antibody (*Depleted* lane), and the extracts were bound to GST-BIR3 fusion protein and analyzed as in *a*. The antibody-bound proteins (*Ab pellet*) were also fractionated and subjected to the same analyses. *Last* lane, 293 cellular extracts were bound to the E314S mutant GST-BIR3 fusion protein, and the bound proteins were analyzed as in *a*. An asterisk indicates nonspecific bands. An arrow indicates the IgG band.

cIAP2 were *in vitro* translated in the presence of [³⁵S]methionine in reticulocyte lysates using MYC-pcDNA3 constructs. Mature Smac or Omi and its mutants were overexpressed in *Escherichia coli* strain BL21(DE3) as C-terminally GST- or His₆-tagged proteins using a pET-28-GST or pET-28 vector, respectively.

Subcellular and Submitochondrial Fractionation—Cells were homogenized in buffer A (20 mM Hepes, pH 7.5, 10 mM KCl, 1.5 mM MgCl₂, 1 mM EDTA, 1 mM EGTA, 250 mM sucrose, 1 mM dithiothreitol, 0.1 mM phenylmethylsulfonyl fluoride, with protease inhibitor mix). The homogenate was centrifuged at 800 × *g*. Nuclei were prepared from the crude nuclear pellet as described before (11). The supernatant was centrifuged at 10,000 × *g*, and the resultant pellet was further processed for mitochondria purification over a Percoll gradient. The postmitochondrial supernatant was subjected to 100,000 × *g*, and the microsomal pellet and cytosolic supernatants were collected separately. Subfractionation of mitochondria by digitonin was carried out as described before (12).

Far Western Blotting—Affinity-purified proteins or cellular extracts were subjected to SDS-PAGE and then transferred to nitrocellulose membrane using a standard Western blotting technique. The proteins on the membrane were probed with ³⁵S-labeled *in vitro* translated XIAP as described before (9).

Cell Death Assays—The ability of Omi to potentiate staurosporine-induced apoptosis (Fig. 4c) was assayed by transfecting human HeLa cells (1 × 10⁵ cells/well) in six-well plates with 0.3 μg of pEGFP-N1 reporter plasmid (CLONTECH), 1.2 μg of empty vector, or a construct encoding C-terminally FLAG-tagged Omi precursor using the LipofectAMINE™ method. Cells were treated with increasing concentrations of staurosporine (0–2.5 μM) for 7 h. Cells were stained with propidium iodide and 4',6-diamidino-2-phenylindole stains. Normal and apoptotic GFP-expressing cells were counted using fluorescence

microscopy. The percentage of apoptotic cells in each experiment was expressed as the mean percentage of apoptotic cells as a fraction of the total number of GFP-expressing cells. The ability of mature Omi to potentiate TRAIL-induced apoptosis (Fig. 6f) was assayed by transfecting human MCF-7 cells (1 × 10⁵ cells/well) in six-well plates with 1.2 μg of GFP-IETD-Omi expression construct or pEGFP-N1 plasmid. 24 h after transfection, cells were treated with TRAIL (0.25 μg/ml) for 16 h, and the percentages of GFP-positive, 4',6-diamidino-2-phenylindole-positive apoptotic cells were determined as above. Similar assays were performed to determine the ability of M-Omi-GFP proteins to induce apoptosis in MCF-7 cells or Apaf^{-/-} or caspase-9^{-/-} mouse embryo fibroblasts.

Immunofluorescence Confocal Microscopy—Cells were grown on coverslips and then stained with a polyclonal antibody raised against pure mature recombinant Omi protein and a mouse anti-Smac monoclonal antibody after fixing the cells with 4% paraformaldehyde. Fluorescein isothiocyanate-conjugated anti-rabbit and rhodamine-conjugated anti-mouse antibodies were used as secondary antibodies. After staining, the coverslips were mounted on slides and observed using confocal microscopy.

In Vitro Interaction Assays—All *in vitro* interactions were performed as described recently (8–10).

RESULTS AND DISCUSSION

To identify novel IAP binding proteins, we used a GST-BIR3 fusion protein as an affinity reagent to purify new IAP-binding proteins from extracts of human 293 cells and mouse tissues. After binding the extracts to the GST-BIR3 protein, the bound proteins were eluted with the IAP-binding motif peptide AVPIA and analyzed by Far Western blotting with ³⁵S-labeled

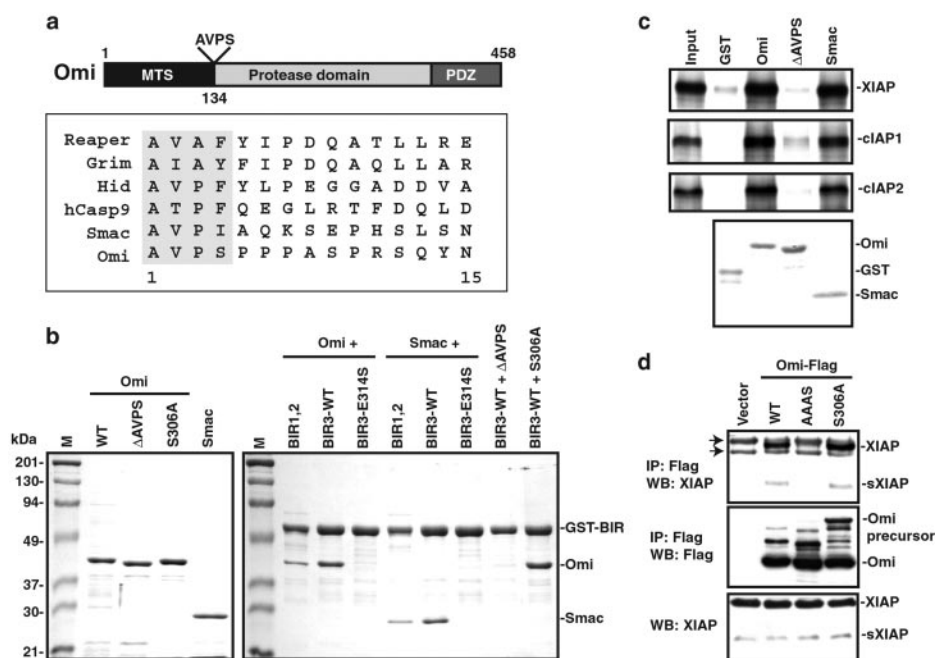


FIG. 2. The N terminus of mature Omi harbors an IAP-binding motif. *a*, bar diagram representing the structure of the Omi precursor and the location of the AVPS motif. *Lower panel*, colinear alignment of the N-terminal sequences of *Drosophila* Reaper, Grim, and Hid and human caspase-9-p12, Smac, and Omi. The IAP-binding motif is highlighted. *b*, *left panel*, Coomassie-stained gel of purified C-terminally His₆-tagged recombinant wild type mature Omi (WT), Omi-ΔAVPS, Omi-S306A, and mature Smac. *Right panel*, The recombinant Omi and Smac proteins were bound to GST-BIR1,2, GST-BIR3, or GST-BIR3-E314S fusion proteins, and the bound proteins were fractionated by SDS-PAGE and stained by Coomassie Blue. *c*, interaction of XIAP, cIAP1, and cIAP2 with mature Omi and Smac. C-terminal His₆-tagged mature Omi, Omi-ΔAVPS, or Smac or GST protein were immobilized onto Talon affinity resin. The bound resins were incubated with *in vitro* translated ³⁵S-labeled XIAP, cIAP1, or cIAP2; washed extensively; and then analyzed by SDS-polyacrylamide gel electrophoresis and autoradiography. GST was used as a negative control (*second lane*). *Fourth panel*, Coomassie-stained gel of the immobilized proteins. *d*, 293T cells were transfected with constructs encoding C-terminal FLAG-tagged Omi wild type or mutant precursors. 36 h after transfection, Omi was immunoprecipitated by FLAG antibody, and the immune complex was analyzed by Western blotting with an XIAP monoclonal antibody (*upper panel*) or FLAG antibody (*middle panel*). *Lower panel*, total extracts probed with the XIAP antibody. A short isoform of XIAP (sXIAP) was also detected with this antibody. The arrows indicate IgG bands.

XIAP. Three proteins, migrating as 23-, 38-, and 80-kDa bands, that specifically interact with the ³⁵S-labeled XIAP, were detected in the AVPIA peptide eluates from the human 293 cells and the mouse tissues (Fig. 1*a*). A large scale affinity preparation was then fractionated on an SDS-polyacrylamide gel (Fig. 1*b*), and the three bands were cut and subjected to microsequencing. Due to the low level of the 80-kDa protein in this preparation, limited N-terminal sequence information was obtained, which was not sufficient for protein identification. The N-terminal sequence information of the other two proteins revealed that the 23-kDa protein is mature Smac/Diablo (13, 14), whereas the 38-kDa band is a previously described serine protease named Omi or Htra2 (15, 16) (GenBank™ accession number XM_002750). Mass spectrometric peptide mass fingerprinting of these two protein bands confirmed the microsequencing results. Furthermore, Western blot analysis of the AVPIA peptide eluates using Smac and Omi antibodies confirmed that the 23-kDa band represents Smac and the 38-kDa band represents Omi (Fig. 1, *a* and *c*).

To confirm that Omi associates directly with the BIR3 domain of XIAP but not with the Smac protein, we depleted Smac from the 293 extracts with a Smac monoclonal antibody, bound the depleted extracts to the GST-BIR3 protein, and then analyzed the bound proteins by Far Western with ³⁵S-XIAP and Western blotting with the Smac antibody. Depletion of Smac did not remove Omi from the 293 extracts, indicating that Omi binds independently to the GST-BIR3 protein (Fig. 1*d*). Moreover, Omi, Smac, and the 80-kDa protein did not bind to the GST-BIR3-E314S mutant (Fig. 1*d*, *last lanes*). This mutation has been shown to abolish binding of Smac and caspase-9 to BIR3 (8, 9, 17). These results indicate that Omi, Smac, and the

80-kDa protein associate directly with the Smac binding pocket on the BIR3 of XIAP.

The BIR3 affinity-purified Omi starts with an amino-terminal AVPS sequence, which represents a conserved IAP-binding motif (Fig. 2*A*). Based on the deduced amino acid sequence of the cloned Omi protein (15, 16), this motif is located at residue 134, suggesting that Omi is made as a precursor protein that undergoes proteolytic processing at residue 133 to remove the N-terminal leader sequence. To determine whether a recombinant Omi lacking the first 133 residues (mature Omi) can interact with the GST-BIR3 fusion protein, we expressed this protein with a C-terminal His₆ tag in bacteria and purified it to apparent homogeneity (Fig. 2*b*, *right panel*). N-terminal amino acid sequencing of the recombinant proteins indicated that the initiator methionine is removed. Both recombinant mature Omi and Smac were able to interact equally with the wild type GST-BIR3 protein but not with the GST-BIR3-E314S mutant (Fig. 2*b*, *left panel*). Mature Omi and Smac were also able to interact with the GST-BIR1,2 fusion protein. Mutation of the active site Ser³⁰⁶ to Ala of mature Omi did not affect its interaction with GST-BIR3. However, deletion of the AVPS motif of mature Omi completely abolished its interaction with the GST-BIR3 fusion protein. Mature Omi can also interact with endogenous XIAP in transfected 293 cells (Fig. 2*d*, *upper panel*) and requires the AVPS motif, since mutation of this motif to AAAS abolished its interaction with the endogenous XIAP. Interestingly, mutation of the AVPS motif to AAAS did not affect the processing and removal of the N-terminal leader sequence of the transfected Omi precursor but completely prevented the interaction with endogenous XIAP (Fig. 2*d*, *middle panel*). *In vitro* interaction assays revealed that mature Omi could also

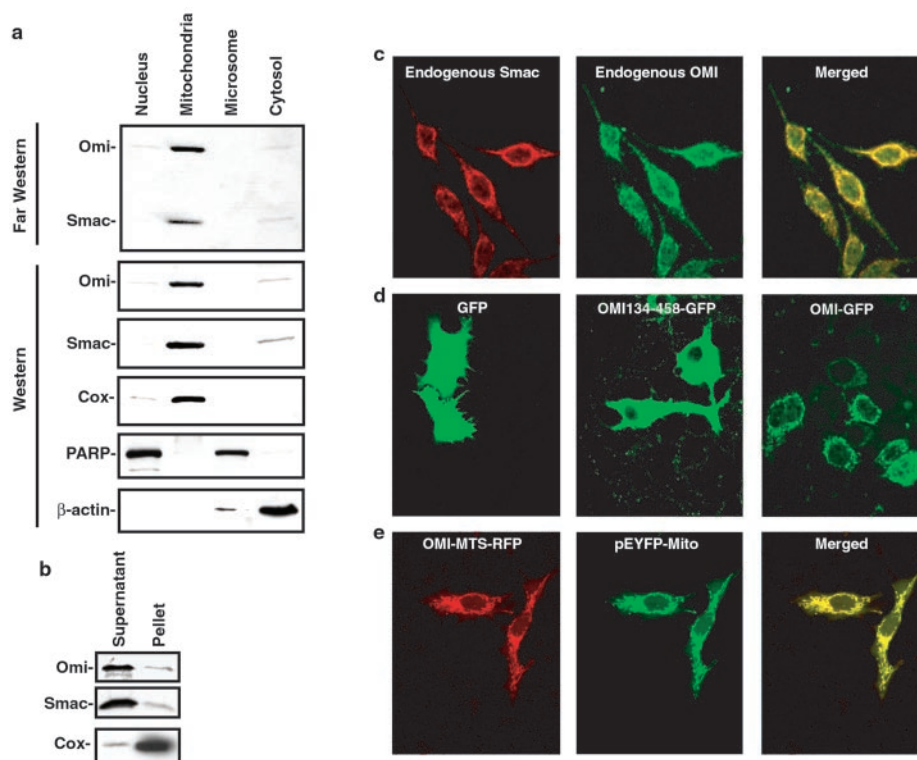


FIG. 3. Omi is localized in the mitochondria. *a*, 293T cells were fractionated into nuclear, mitochondrial, microsomal, and cytosolic fractions. The nuclear, mitochondrial, and microsomal fractions were lysed in a hypotonic buffer, and the soluble proteins bound to GST-BIR3 fusion protein and were analyzed as in the legend to Fig. 1*a*. The same Far Western blot (upper panel) was then probed with Omi and Smac antibodies (second and third panels, respectively). Total subcellular fractions were also immunoblotted with antibodies against cytochrome *c* oxidase (fourth panel), poly(ADP-ribose) polymerase (fifth panel), and β -actin (sixth panel). *b*, purified mitochondria from 293 cells were treated with a buffer containing 1.2% digitonin, and the supernatant and mitoplasts (pellet) were then analyzed by Western blotting with Omi, Smac, and cytochrome *c* oxidase antibodies. *c*, immunofluorescence confocal microscopy of MCF-7 cells stained with Omi-specific (middle panel, green) and Smac-specific (left panel, red) antibodies. *d*, confocal micrographs of MCF-7 cells transfected with GFP (left panel) or C-terminal GFP-tagged mature Omi (Omi134–458-GFP; middle panel) or Omi precursor (Omi-GFP; right panel). *e*, confocal micrographs of MCF-7 cells transfected with C-terminal RFP-tagged Omi1–60 (Omi-MTS-RFP; left panel) and pEYFP-Mito marker (middle panel). The right panels in *c* and *e* represent merged micrographs.

interact with cIAP1 and cIAP2 (Fig. 2*c*). The above data indicate that Omi is a *bona fide* IAP-binding protein with an N-terminal IAP binding motif essential for its ability to bind IAPs.

Computer analysis using the PSORT program revealed that the N-terminal leader sequence of the Omi precursor contains within its first 60 residues a typical mitochondrial targeting sequence. This sequence might be removed by mitochondrial processing peptidases upon import into the mitochondria. To examine whether the endogenous mature Omi protein is indeed localized in the mitochondria, we subfractionated 293 cells into cytosolic, mitochondrial, microsomal, and nuclear fractions and bound each fraction to the GST-BIR3 protein. As shown in Fig. 3*a*, Far Western and Western blot analyses with ^{35}S -XIAP and Smac and Omi antibodies, respectively, showed the majority of Omi and Smac to be localized in the mitochondrial fraction. Next we subfractionated purified mitochondria from HEK293 cells into intermembrane space and matrix fractions using 1–1.2% digitonin, which specifically disrupts the outer mitochondrial membrane without affecting the inner mitochondrial membrane. The fractions were analyzed by immunoblotting with Omi and Smac antibodies. Both Omi and Smac were predominantly present in the intermembrane space fraction (Fig. 3*b*).

Immunofluorescence confocal microscopy of MCF-7 cells stained with Omi- and Smac-specific antibodies revealed that the endogenous Omi and Smac proteins colocalize with each other and exhibit punctate perinuclear staining characteristic of mitochondrial localization (Fig. 3*c*). To confirm the mitochondrial localization of Omi, we transfected MCF-7 cells with a

C-terminal GFP-tagged Omi precursor construct. The ectopically transfected Omi precursor exhibited punctate mitochondrial fluorescence (Fig. 3*d*, right panel). The removal of the mitochondrial targeting sequence of Omi resulted in the expression of mature Omi (residues 134–458) in the cytoplasm (Fig. 3*d*, middle panel). The first 60 residues of the Omi precursor, which harbors the MTS, was sufficient for targeting RFP to the mitochondria when expressed as a fusion protein with RFP (Fig. 3*e*). Taken together, the above data indicate that Omi colocalizes with Smac in the intermitochondrial membrane space.

To determine whether Omi is released together with Smac and cytochrome *c* from the mitochondria to the cytoplasm during apoptosis, we treated Jurkat and HL-60 cells with staurosporine, which is known to induce the mitochondrial apoptotic pathway, and analyzed their cytosolic extracts by immunoblot analysis. As shown in Fig. 4*a*, cytochrome *c*, Smac, and Omi accumulated in the cytosol of these cells in a time-dependent manner after treatment with staurosporine. Processing of procaspase-3 also followed a similar time course, with maximum processing observed at 6–8 h after treatment. Very little or no Omi or Smac proteins nor processing of procaspase-3 was detected in the extracts at zero time points. Similar results were obtained after treatment of Jurkat cells with TRAIL (Fig. 4*b*). Immunofluorescence confocal microscopy of staurosporine-treated HeLa cells or TRAIL-treated MCF-7 cells showed diffused immunofluorescence staining of Omi, whereas in the untreated control cells it is mostly punctate and perinuclear (Fig. 4*c*). The above data clearly show that Omi is released together with cytochrome *c* and Smac during apoptosis.

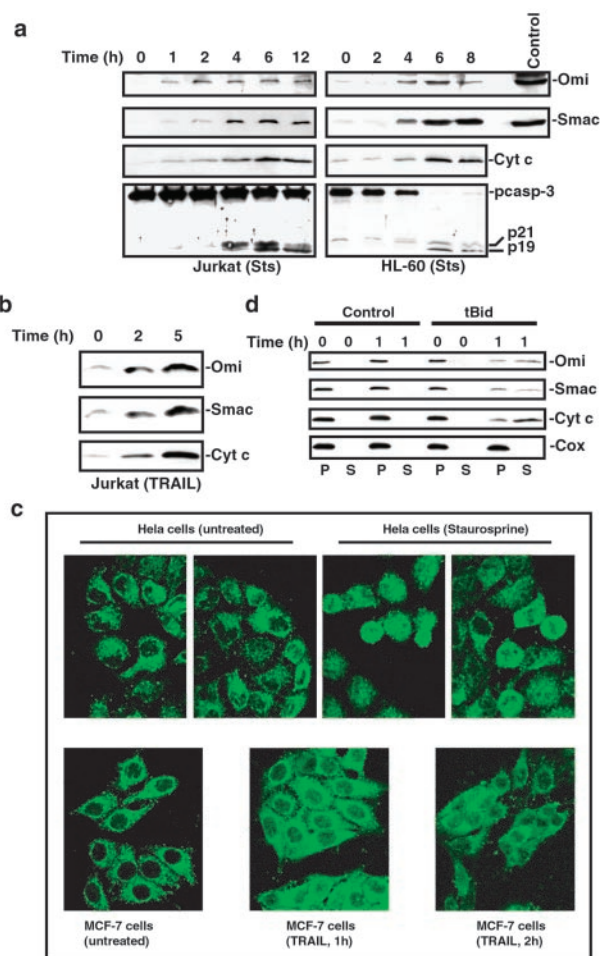


FIG. 4. Omi is released together with Smac and cytochrome *c* from the mitochondria during apoptosis. *a*, human Jurkat T-cells and HL-60 cells were treated with staurosporine (2 μ M) for the indicated periods of time, the cells were collected and lysed, the cytosolic extracts were bound to GST-BIR3, and the bound proteins were analyzed by immunoblotting with Omi and Smac antibodies (*first* and *second panel*, respectively). The cytosolic extracts were also analyzed by immunoblotting with cytochrome *c* (*third panel*) or caspase-3 (*fourth panel*) antibodies. *b*, Jurkat cells were treated with TRAIL (1 μ g/ml) for the indicated periods of time; the cells were collected and lysed; and the cytosolic extracts were analyzed by immunoblotting with Omi, Smac, and cytochrome *c* antibodies. *c*, immunofluorescence confocal microscopy of untreated or staurosporine-treated (1 μ M, 5 h) HeLa cells or untreated or TRAIL-treated (1 μ g/ml) MCF-7 cells stained with Omi-specific antibody. Note the punctate perinuclear staining in the untreated cells and the diffused staining in the treated cells. *d*, isolated 293 mitochondria were incubated with or without purified tBid (350 nM) as indicated. The supernatants (S) and mitochondrial pellets (P) were separated by centrifugation and analyzed by immunoblotting with Omi, Smac, cytochrome *c*, and cytochrome *c* oxidase antibodies.

The ability of TRAIL to induce release of Omi from the mitochondria of MCF-7 and Jurkat cells suggests that tBid, which is generated by active caspase-8 after TRAIL-receptor ligation, is responsible for the release of Omi. To test this hypothesis, we incubated isolated mitochondria with a physiological amount of tBid. As shown in Fig. 4*d*, tBid induced release of Omi, Smac, and cytochrome *c* from the mitochondria into the supernatants. Combined, the above data clearly show that Omi is released from the mitochondria together with cytochrome *c* and Smac during apoptosis and after stimulation of mitochondria with tBid.

Next, we determined whether Omi, like Smac, promotes caspase-9 activity in HEK293 S100 extracts in the presence of XIAP. To measure the caspase-9 activity in these extracts, we added 35 S-labeled procaspase-3 to the S100 extracts and stim-

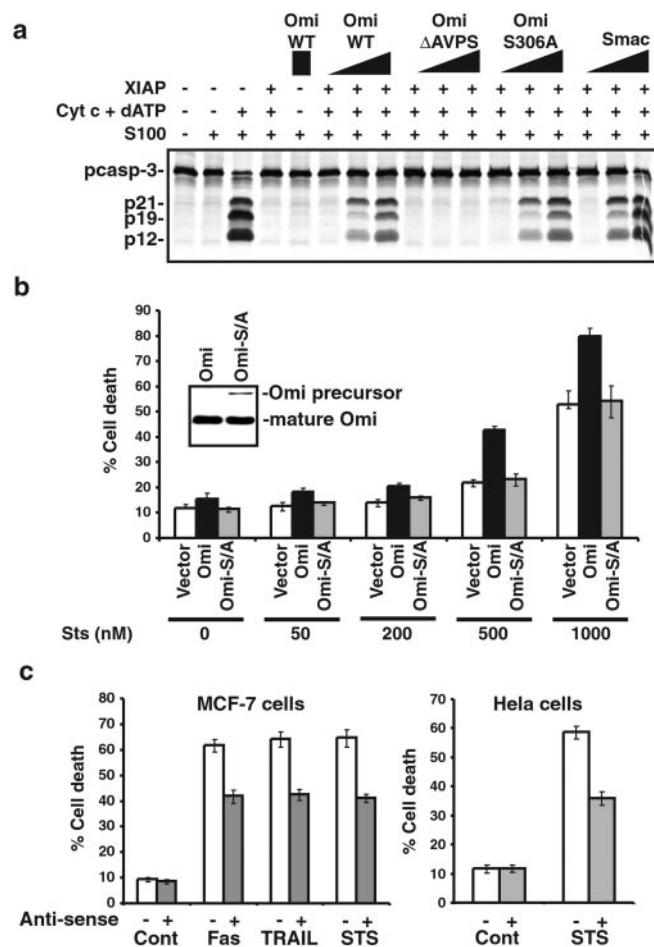


FIG. 5. Omi can potentiate caspase activation and apoptosis. *a*, 293T S100 extracts (20 μ g) were mixed with purified XIAP (50 ng) and then stimulated with cytochrome *c* (0.5 μ g) plus dATP (1 mM) in the presence of increasing amounts (10, 50, and 300 ng, respectively) of purified mature WT Omi, Omi- Δ AVPS, Omi-S306A, or mature Smac in a 10- μ l reaction volume. S100 extracts without XIAP (-) were used as controls. The reactions were carried out in the presence of 35 S-labeled procaspase-3 for 1 h and then analyzed by SDS-polyacrylamide gel electrophoresis and autoradiography. *Fifth lane*, S100 extracts incubated with 300 ng of WT Omi without XIAP. *b*, HeLa cells were transfected with an empty vector or constructs encoding a C-terminally FLAG-tagged wild type- or S306A Omi precursor together with pEGFP-N1 plasmid (CLONTECH) at a 4:1 ratio. The AVPS motif in the S306A mutant Omi precursor is also mutated to the VVAS sequence to prevent binding to IAPs. 24 h after transfection, the cells were treated with the indicated doses of staurosporine for 5 h, and the percentages of GFP-positive apoptotic cells were determined. *Inset*, expression of mature Omi wild type and Omi S306A mutant in the transfected cells as determined by immunoblotting with FLAG antibody. *c*, MCF-7 and HeLa cells were transfected with a full-length antisense Omi cDNA (+) in a pRSC-GFP double expression vector or an empty pRSC-GFP vector (-). 72 h after transfection, the cells were treated with Fas (500 ng/ml, 5 h), TRAIL (1 μ g/ml, 5 h), or staurosporine (1 μ M, 5 h) as indicated, and the percentages of GFP-positive apoptotic cells were determined by fluorescent microscopy after staining with 4',6-diamidino-2-phenylindole and propidium iodide.

ulated the extracts with cytochrome *c* and dATP. As shown in Fig. 5*a*, mature WT Omi or the S306A mutant was able to promote procaspase-3 activation in the XIAP-containing S100 extracts almost to the same extent as Smac. The ability to potentiate procaspase-3 activation was dependent on the AVPS motif of Omi, since deletion of this motif abolished its caspase-promoting activity. These observations suggest that Omi, like Smac, is able to disrupt the interaction of caspase-9 with XIAP in the S100 extracts to promote procaspase-3 activation.

To determine whether release of Omi can potentiate apopto-

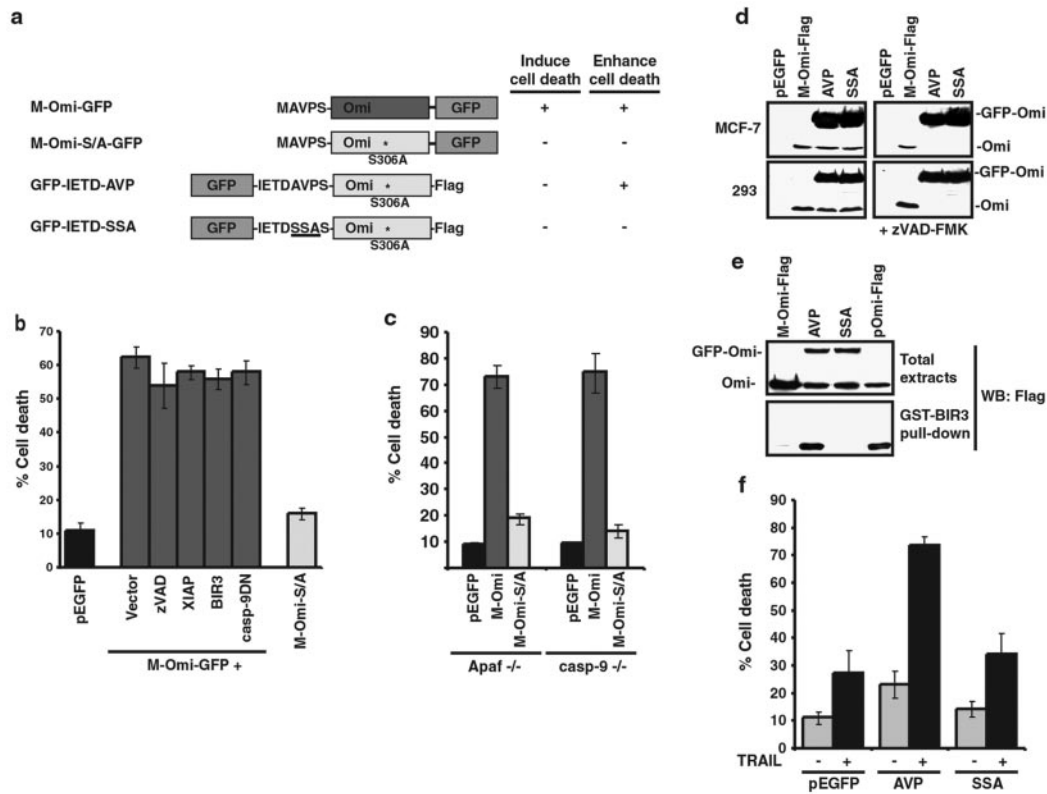


FIG. 6. Dual role of Omi in cell death. *a*, schematic diagrams of the Omi-GFP and GFP-IETD-Omi constructs used to assay the ability of Omi to induce apoptosis or to enhance apoptosis by other stimuli. The Omi fusion proteins that induce or enhance apoptosis are marked with a *plus sign*, and those that do not are marked with a *minus sign*. *b*, MCF-7 cells were transfected with M-Omi-S/A-GFP or pEGFP-N1 alone or M-Omi-GFP together with empty vector or expression construct encoding XIAP, XIAP-BIR3, or caspase-9DN. The cells were also transfected with the M-Omi-GFP expression construct in the presence of zVAD-FMK (20 μ M). 36 h after transfection, the percentages of apoptotic cells were determined as described under “Experimental Procedures.” *c*, Apaf-1^{-/-} or caspase-9^{-/-} mouse embryo fibroblasts were transfected with pEGFP-N1, M-Omi-GFP, or M-Omi-S/A-GFP. 36 h after transfection, the percentages of apoptotic cells were determined. *d*, MCF-7 and 293T cells were transfected with pEGFP or M-Omi-Flag, GFP-IETD-AVP (AVP), or GFP-IETD-SSA (SSA) expression constructs in the presence or absence of zVAD-FMK (20 μ M). 24 h after transfection, the cells were harvested, and their extracts were fractionated and analyzed by immunoblotting with FLAG-horseradish peroxidase antibody. M-Omi-FLAG is similar to the M-Omi-GFP shown in *a*, except that the GFP tag was replaced with FLAG tag. *e*, 293T cells were transfected with the indicated expression constructs. 24 h after transfection, the cells were transfected with GST-BIR3. The extracts and the precipitated proteins were immunoblotted with FLAG-horseradish peroxidase antibody. *pOmi-FLAG*, C-terminal FLAG-tagged Omi precursor (only the mature Omi can be seen). *f*, MCF-7 cells were transfected with the indicated expression constructs. 24 h after transfection, the cells were left untreated (-) or treated with TRAIL (+) for 16 h. The percentage of round apoptotic cells was determined.

sis, we transfected human HeLa cells with the Omi precursor and stimulated the cells with different doses of staurosporine. We reasoned that treatment with staurosporine should enhance the overexpressed Omi from the mitochondria, thereby enhancing apoptosis. As shown in Fig. 5*b*, transiently expressed wild type Omi did not induce significant apoptosis in the absence of staurosporine. However, at 500 nM staurosporine, ~43% of the Omi-transfected cells showed signs of apoptosis compared with ~20% in the case of the vector-transfected cells. With higher concentrations of staurosporine, increased apoptosis was observed in the Omi-transfected cells compared with the vector-transfected cells. No apoptosis potentiation was observed with an active site Omi precursor mutant, which also has a mutant VVAS sequence instead of the AVPS motif. These observations suggest that release of Omi by an apoptotic stimulus such as staurosporine enhances cell death.

To determine whether endogenous Omi plays a role in cell death, we transfected MCF-7 and HeLa cells with an antisense Omi cDNA to reduce the expression of Omi in the transfected cells. As shown in Fig. 5*c*, the Omi antisense cDNA reduced significantly (30–35%) the sensitivity of the transfected cells to apoptotic stimuli. These results suggest that Omi participates together with other apoptotic factors in the overall sensitivity of cells to apoptosis.

Since Omi possesses both serine protease and IAP binding

activities, we wanted to determine the contribution of each of these activities separately toward its overall proapoptotic activity. To determine the contribution of the serine protease activity of Omi toward its proapoptotic activity, it was necessary to express cytosolic protease-active and -inactive forms of Omi that do not bind IAPs in cells. This was achieved by expressing active and inactive (S306A) Omi-GFP fusion proteins without the MTS (M-Omi-GFP and M-Omi-S/A-GFP, respectively) in MCF-7 cells (Fig. 6*a*). We found that these forms of Omi do not bind XIAP-BIR3 (Fig. 6*e*, *first lane*) because the initiator methionine before the AVPS motif is not removed in transfected human cells (not shown). Nevertheless, only the serine protease-active M-Omi-GFP, but not the inactive M-Omi-S/A-GFP, was able to induce cell death in MCF-7 cells (Fig. 6*b*). Similar results were obtained with cytosolic Omi variants lacking the AVPS motif (data not shown). Of note, the Omi-killing activity was independent of the cellular caspase activity, since inhibition of cellular caspases with zVAD-FMK, XIAP, XIAP-BIR3, or caspase-9-DN did not block the ability of M-Omi-GFP to kill these cells. Consistent with these results, M-Omi-GFP was also able to induce cell death in Apaf^{-/-} and caspase-9^{-/-} mouse embryo fibroblasts (Fig. 6*c*). These results indicate that Omi can induce cell death in mammalian cells independent of caspases, Apaf-1, or IAPs via its serine protease activity.

We next tested the contribution of the IAP binding activity of Omi to its killing activity. To do that, we replaced the MTS of Omi with a GFP-IETD sequence and mutated its active site Ser³⁰⁶ to Ala (Fig. 6a, GFP-IETD-AVP). Of note, the presence of the IETD sequence between GFP and Omi-S/A allowed caspase-dependent cleavage at the IETD site after the Asp residue and release of mature Omi-S/A in the cytosol of the transfected 293 and MCF-7 cells (Fig. 6d). This mature Omi-S/A was able to bind the GST-BIR3 fusion protein (Fig. 6e), indicating that it is correctly processed to expose its AVPS motif. Consistent with this result, very little or no processing at the IETD site was observed in the cytosolic extracts of these cells in the presence of the pancaspase inhibitor zVAD-FMK (Fig. 6d). As shown in Fig. 6f, expression of the GFP-IETD-AVP fusion protein in MCF-7 cells enhanced TRAIL-induced apoptosis in these cells severalfold above the GFP-transfected control cells. This activity was dependent on the AVPS motif, since mutation of the AVPS motif to an SSAS motif (GFP-IETD-SSA) abolished the apoptotic enhancement activity of Omi-S/A and the ability to bind to BIR3. These results indicate that the IAP binding activity of Omi represented by its AVPS motif plays a significant role in its ability to potentiate apoptosis independent of its protease activity. Taken together, Omi not only can induce cell death through its serine protease activity but also via its ability to bind and neutralize IAPs.

Our observations reveal a new level of regulation of apoptosis by the mitochondria. The identification of Omi as a mitochondrial serine protease that can also bind and neutralize IAPs adds to the list of proapoptotic proteins such as cytochrome *c*, apoptosis-inducing factor, Smac, and endonuclease G (18–21), which are released from the mitochondria during apoptosis, and emphasizes the importance of the mitochondria in the cell death pathway of eukaryotic cells. Because Omi is a serine protease, its sequestration in the mitochondria protects healthy cells from its proteolytic activity. However, when cells become damaged, they release Omi, together with other inter-mitochondrial membrane space proteins, into the cytoplasm, where it could cause irreparable proteolytic damage to important structural and regulatory components of the cell. In addition, mature Omi could play a role as an IAP inhibitor in the caspase-dependent apoptotic pathway by binding to the BIR3 domain of XIAP and disrupting its interaction with the activated caspase-9. This activity may complement the activity of Smac by neutralizing more IAPs in the cytoplasm, resulting in more caspase activation in cells undergoing apoptosis.

While the importance of caspases in cell death is well established, a large body of evidence suggests that other types of proteases might also be important (22, 23). For example, inhibitors of serine proteases such as diisopropyl fluorophosphate, 1-chloro-3-tosylamido-7-amino-2-heptanone, and L-1-tosylamido-2-phenylethyl chloromethyl ketone can delay or fully inhibit distinct steps of the cell death pathway (22, 24). Moreover, inhibition of caspases generally delays but does not completely block cell death by some cell death stimuli. Thus, the serine protease activity of Omi could be responsible for the noncaspase-dependent cell death observed in many model systems.

Although there is now clear evidence that cytochrome *c*, apoptosis-inducing factor, and endonuclease G contribute to

the demise of the cell when released from the mitochondria into the cytoplasm or nucleus, the real physiological function of these proteins is far from being killer proteins. In fact, these proteins are essential for normal mitochondrial function and cell survival. This is most likely true for Omi. Omi belongs to the heat shock response serine proteases (HtrAs), which have been shown in bacteria to be essential for cell survival at high temperature (25). Omi and its related family members could control protein stability and turnover under thermal, osmotic, pH, and other stress conditions. Interestingly, an Omi-related protease has been identified in the chloroplast of *Arabidopsis thaliana*, suggesting that these proteases play important roles in organellar biogenesis and function (26). Although our data clearly show that Omi is localized predominantly in the mitochondria, recent data indicated that Omi is also localized in the nucleus of stressed cells (16), suggesting that Omi perhaps could translocate from mitochondria to the nucleus after stress.

In conclusion, the release of Omi from the mitochondria might represent a novel cell death pathway that has not yet been fully appreciated. Omi could bind and inhibit the cellular IAPs, thus potentiating the caspase-dependent apoptotic pathway. More importantly, Omi could induce cell death independent of caspases via its serine protease activity. The targeted disruption of the Omi gene in the future should allow the determination of the precise role of Omi in cell death and survival.

REFERENCES

1. Miller, L. K. (1999) *Trends Cell Biol.* **9**, 323–328
2. Deveraux, Q. L., and Reed, J. C. (1999) *Genes Dev.* **13**, 239–252
3. Reed, J. C., and Bischoff, J. R. (2000) *Cell* **102**, 545–548
4. Deveraux, Q. L., Takahashi, R., Salvesen, G. S., and Reed, J. C. (1997) *Nature* **388**, 300–304
5. Abrams, J. M. (1999) *Trends Cell Biol.* **9**, 435–440
6. Vucic, D., Kaiser, W. J., and Miller, L. K. (1998) *Mol. Cell. Biol.* **18**, 3300–3309
7. Goyal, L., McCall, K., Agapite, J., Hartwig, E., and Steller, H. (2000) *EMBO J.* **19**, 589–597
8. Wu, G., Chai, J., Suber, T. L., Wu, J. W., Du, C., Wang, X., and Shi, Y. (2000) *Nature* **408**, 1008–1012
9. Srinivasula, S. M., Hegde, R., Saleh, A., Datta, P., Shiozaki, E., Chai, J., Lee, R. A., Robbins, P. D., Fernandes-Alnemri, T., Shi, Y., and Alnemri, E. S. (2001) *Nature* **410**, 112–116
10. Srinivasula, S. M., Datta, P., Fan, X. J., Fernandes-Alnemri, T., Huang, Z., and Alnemri, E. S. (2000) *J. Biol. Chem.* **275**, 36152–36157
11. Martin, S. J., Newmeyer, D. D., Mathias, S., Farschon, D. M., Wang, H. G., Reed, J. C., Kolesnick, R. N., and Green, D. R. (1995) *EMBO J.* **14**, 5191–5200
12. Greenawald, J. W. (1974) *Methods Enzymol.* **31**, 310–323
13. Du, C., Fang, M., Li, Y., Li, L., and Wang, X. (2000) *Cell* **102**, 33–42
14. Verhagen, A. M., Ekert, P. G., Pakusch, M., Silke, J., Connolly, L. M., Reid, G. E., Moritz, R. L., Simpson, R. J., and Vaux, D. L. (2000) *Cell* **102**, 43–53
15. Faccio, L., Fusco, C., Chen, A., Martinotti, S., Bonventre, J. V., and Zervos, A. S. (2000) *J. Biol. Chem.* **275**, 2581–2588
16. Gray, C. W., Ward, R. V., Karran, E., Turconi, S., Rowles, A., Viglienghi, D., Southan, C., Barton, A., Fantom, K. G., West, A., Savopoulos, J., Hassan, N. J., Clinkenbeard, H., Hanning, C., Amegadzie, B., Davis, J. B., Dingwall, C., Livi, G. P., and Creasy, C. L. (2000) *Eur. J. Biochem.* **267**, 5699–5710
17. Liu, Z., Sun, C., Olejniczak, E. T., Meadows, R. P., Betz, S. F., Oost, T., Herrmann, J., Wu, J. C., and Fesik, S. W. (2000) *Nature* **408**, 1004–1008
18. Kroemer, G., and Reed, J. C. (2000) *Nat. Med.* **6**, 513–519
19. Ferri, K. F., and Kroemer, G. (2001) *Bioessays* **23**, 111–115
20. Li, L. Y., Luo, X., and Wang, X. (2001) *Nature* **412**, 95–99
21. Parrish, J., Li, L., Klotz, K., Ledwich, D., Wang, X., and Xue, D. (2001) *Nature* **412**, 90–94
22. Solary, E., Eymin, B., Droin, N., and Haug, M. (1998) *Cell. Biol. Toxicol.* **14**, 121–132
23. Johnson, D. E. (2000) *Leukemia* **14**, 1695–1703
24. Higuchi, M., Singh, S., Chan, H., and Aggarwal, B. B. (1995) *Blood* **86**, 2248–2256
25. Spiess, C., Beil, A., and Ehrmann, M. (1999) *Cell* **97**, 339–347
26. Itzhaki, H., Naveh, L., Lindahl, M., Cook, M., and Adam, Z. (1998) *J. Biol. Chem.* **273**, 7094–7098

Identification of Omi/HtrA2 as a Mitochondrial Apoptotic Serine Protease That Disrupts Inhibitor of Apoptosis Protein-Caspase Interaction

Ramesh Hegde, Srinivasa M. Srinivasula, ZhiJia Zhang, Richard Wassell, Rula Mukattash, Lucia Cilenti, Garrett DuBois, Yuri Lazebnik, Antonis S. Zervos, Teresa Fernandes-Alnemri and Emad S. Alnemri

J. Biol. Chem. 2002, 277:432-438.

doi: 10.1074/jbc.M109721200 originally published online October 17, 2001

Access the most updated version of this article at doi: [10.1074/jbc.M109721200](https://doi.org/10.1074/jbc.M109721200)

Alerts:

- [When this article is cited](#)
- [When a correction for this article is posted](#)

[Click here](#) to choose from all of JBC's e-mail alerts

This article cites 26 references, 7 of which can be accessed free at <http://www.jbc.org/content/277/1/432.full.html#ref-list-1>